Approximate relationship between frequency-dependent skin depth resolved from geoelectromagnetic pedotransfer function and depth of investigation resolved from geoelectrical measurements: A case study of coastal formation, southern Nigeria

N J George[1,*], D N Obiora[2], A M Ekanem[1] and A E Akpan[3]

[1]*Department of Physics, Akwa Ibom State University, Ikot Akpaden, PMB 1169, Uyo, Akwa Ibom State, Nigeria.*
[2]*Department of Physics and Astronomy, University of Nigeria, Nsukka, Nigeria.*
[3]*Department of Applied Geophysics Programme, Department of Physics, University of Calabar, Calabar, Nigeria.*
[*]*Corresponding author. e-mail: nyaknojimmyg@gmail.com; nyaknogeorge@aksu.edu.ng*

The task involved in the interpretation of Vertical Electrical Sounding (VES) data is how to get unique results in the absence/limited number of borehole information, which is usually limited to information on the spot. Geological and geochemical mapping of electrical properties are usually limited to direct observations on the surface and therefore, conclusions and extrapolations that can be drawn about the system electrical characteristics and possible underlying structures may be masked as geology changes with positions. The electrical resistivity study pedotransfer functions (PTFs) have been linked with the electromagnetic (EM) resolved PTFs at chosen frequencies of skin/penetration depth corresponding to the VES resolved investigation depth in order to determine the local geological attributes of hydrogeological repository in the coastal formation dominated with fine sand. The illustrative application of effective skin depth depicts that effective skin depth has direct relation with the EM response of the local source over the layered earth and thus, can be linked to the direct current earth response functions as an aid for estimating the optimum depth and electrical parameters through comparative analysis. Though the VES and EM resolved depths of investigation at appropriate effective and theoretical frequencies have wide gaps, diagnostic relations characterising the subsurface depth of interest have been established. The determining factors of skin effect have been found to include frequency/period, resistivity/conductivity, absorption/attenuation coefficient and energy loss factor. The novel diagnostic relations and their corresponding constants between 1-D resistivity data and EM skin depth are robust PTFs necessary for checking the accuracy associated with the non-unique interpretations that characterise the 1-D resistivity data, mostly when lithostratigraphic data are not available.

1. Introduction

In electromagnetic prospecting, electrical conductivity, the inverse of electrical resistivity of the earth, plays a pivotal role in the penetration that can be obtained. Generally, in geophysical studies that involve electric current, pedotransfer functions of electric and magnetic soil properties governed by Maxwell's equations (a set of partial differential equations that relate the electromagnetic properties

Keywords. 1-D electrical resistivity; skin depth; depth of penetration; depth of investigation; theoretical and effective frequencies.

to the earth's properties) are often efficient in resolving and predicting the earth's convoluted properties. Estimating the depth of investigation of an electromagnetic (EM) system is paramount in survey design and data interpretation of subsurface conducting media (Singh and Mogi 2003a). The skin depth permits the characterisation of the depth of investigation, which increases with the square root of the product of medium average resistivity and period (inverse of frequency). Though it was originally defined for homogeneous media, its usage has been extended to heterogeneous cases of geological formations as well. It is generic that EM field at any frequency is present at all the subsurface depths even though it may be infinitesimally small (Singh and Mogi 2003b). Practically, the depth of investigation from a geophysical point of view is predicated on factors that include lithostratigraphic contents, precision and accuracy of equipment, and signal-to-noise ratio level (Spies 1989; Singh and Mogi 2003b). Certainty in the estimation of depth of investigation in layered earth sections is always marred by the skin effect of the conducting media, and as such integrated approaches have been posited by many earth's researchers (Keller 1971; Bostick 1977; Parker 1982; Spies 1989; Reid and Macnae 1999) to make good, the estimated depth of burial of the suspected geo-resource. The method relating skin depth to effective depth of penetration of EM fields in the earth (Bostick 1977), and the effective skin depth (Reid and Macnae 1999) are based on the concept of skin depth, which also affects depth of investigation involving direct current electrical resistivity measurements leading to the estimation of depth of burial of geo-resource of interest. The skin depth is connected to plane wave electromagnetic field, which is commonly employed in the estimation of depth of investigation of electromagnetic prospecting system. The usefulness of the skin depth concept is reflected in the representation of the maximum depth of investigation of an EM method operating at average frequency (f) of subsurface down to that depth of known average resistivity (ρ)/conductivity (σ) from the top layer (Hersir and Flóvenz 2013). The skin depth (ς_T) is defined as the depth at which the amplitude of the plane-wave electric or magnetic field in a homogeneous half-space falls to e^{-1} (nearly 37%) of its surface value (Stratton 1941), while the phase rotates by one radian (Spies 1989). The theoretical skin depth is expressed as:

$$\varsigma_T = \frac{503.3}{\sqrt{f\sigma}}, \tag{1}$$

where σ is the conductivity and f is the propagating frequency of the electric current into the subsurface. The expression in equation (1) shows that the theoretical skin depth of EM wave is inversely proportional to both the frequency and subsurface conductivity. Practically, the effective skin depth (ς_{eff}) can be regarded as local source skin depth (LSSD), which is described as the depth at which the amplitude of the electric or magnetic field of a local finite source in a homogeneous half-space reduces to e^{-1} of its surface value. This practical depth is a maximum depth at which a conductor may lie and still produce a recognizable electric or magnetic anomaly. It is about one-fifth of the theoretical depth (Kearey and Brooks 2002). Thus the relationship between the theoretical and the practical effective depth is given as:

$$\varsigma_{\text{eff}} \approx \frac{1}{5}\varsigma_T \approx \frac{100}{\sqrt{f\sigma}}. \tag{2}$$

This, on the average shows that the theoretical skin depth in EM induction is five times the effective depth of penetration. According to Beer's law (Schuylenbergh and Puers 2009), rate of fall of current intensity I can be described by this exponential law known as:

$$I(z) = I_s e^{-\alpha Z}, \tag{3}$$

where I, I_s, α and z represent decayed current, surface current, frequency dependent absorption coefficient/attenuation factor and total depth. The attenuation of magnetic or electric signal is the major cause of energy loss in geological formations. The absorption/attenuation factor (α) principally depends on the electric conductivity (σ), magnetic permeability (μ) and dielectric (ε) properties of the geological unit through which the signal is propagating as well as the frequency of the signal itself. In non-magnetic geological formations, attenuation factor is given by the expression (Parasnis 1979; Karim and Al-dami 2012):

$$\begin{aligned}\alpha &= \omega\left\{\frac{\mu\varepsilon}{2}\left[\left(1+\frac{\sigma^2}{\omega^2\varepsilon^2}\right)^{\frac{1}{2}}-1\right]\right\}^{\frac{1}{2}}\\ &= \omega\left\{\frac{\mu\varepsilon}{2}\left[\left(1+\Gamma^2\right)^{\frac{1}{2}}-1\right]\right\}^{\frac{1}{2}},\end{aligned} \tag{4}$$

where $\omega = 2\pi f$, f is the frequency (Hz), μ is the magnetic permeability ($4\pi \times 10^{-7}$H/m), σ in (S/m), is the bulk conductivity at the given frequency, ($\varepsilon = \varepsilon_r\varepsilon_o$) is the permittivity, ($\varepsilon_o$) is the permittivity of free space (8.854×10^{-12}F/m) and ε_r is the relative permittivity. The ratio ($\sigma/\omega\varepsilon$) in the above expression signifies the loss factor denoted as Γ in Siemens-second per metre. Going by (4), the penetration depth, ς_T, relates to the

absorption/attenuation coefficient by the expression in equation (5),

$$\varsigma_T = \frac{1}{\alpha}. \tag{5}$$

Since the power of a wave in a particular medium is proportional to the *square* of a field quantity, one may speak of a penetration depth at which the magnitude of the electric (or magnetic) field has decayed to e^{-1} of its surface value, and at which point the power of the wave has therefore decreased to e^{-2} or about 14% of its surface value.

The alternating current density J in a geological formation decreases exponentially from its value at the surface, J_S, through the depth, d, from the surface, as follows:

$$J = J_s e^{-d/\varsigma_T}. \tag{6}$$

In terms of current density, the skin depth is also defined as the depth below the surface of the geologic formation at which the current density has fallen to e^{-1} (about 37%) of J_s, the surface current density. The skin depth is thus also defined as the depth below the surface of the conductor at which the current density has fallen to e^{-1} (about 37%) of J_s. The determination of the layer effective skin depth of penetration from the existing empirical relations of frequency-dependent, alternating, electric current sources can be related to the depth of penetration resolved from direct current resistivity measurements at the frequency of the alternating current source. The reason for the possibility of this correlation is based on the fact that the formation resistivity or its converse, the conductivity of the subsurface accessed by either the alternating or a direct current source is the same. This novel idea of correlating the effective skin depth and the supposed depth of penetration of geo-resource of interest by electric current may be technically necessary in resolving artefacts encountered in electrical resistivity measurements.

2. Geological setting of the VES data used for correlations

The geology of the coastal area considered in this study is the Pleistocene Coastal Plain Sands (CPS) (also known as the Benin Formation) and alluvium environments of the Niger Delta region of southern Nigeria (figure 1). The Benin Formation which overlies the Parallic Agbada Formation covers over 80% of the study area (Edet and Worden 2000; George *et al.* 2011a, b). The Benin Formation sediments are characterised by interfringing units of lacustrine and fluvial loose sands, pebbles, clays and lignite streaks of varying thicknesses. The alluvial units compose of tidal and fluvial sediments, beach sands and soils (Reijers and Petters 1988; Reijers *et al.* 1999; Akpan *et al.* 2000; George *et al.* 2011a, b), which are mostly found in the southern parts and along the riverbanks. The CPS, which is fraught with argillaceous material in some locations, is covered by thin lateritic overburden materials with varying thicknesses at some places but is massively exposed near the shorelines (George *et al.* 2014a, b, 2015). The CPS forms the major groundwater repositories in the area. This geological formation is intercalated with poorly sorted continental (fine-medium-coarse) sands and gravels

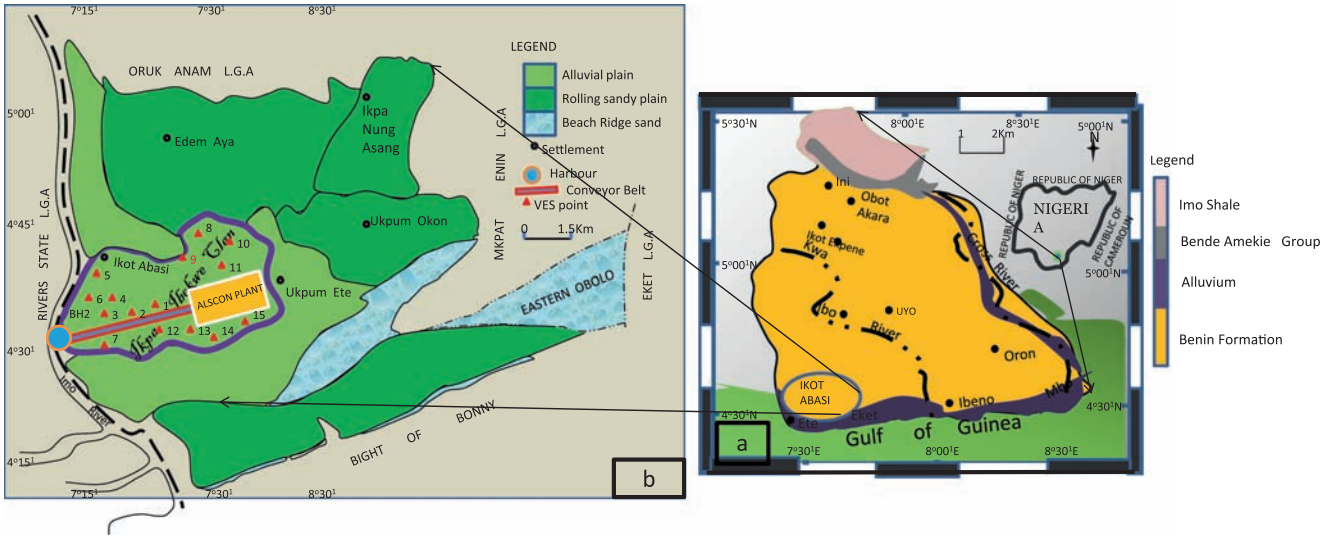

Figure 1. (**a**) Schematic geologic map of Akwa Ibom State in southern Nigeria showing Ikot Abasi. (**b**) Map of Ikot Abasi L.G.A. showing the considered locations in dark blue with VES points and boreholes for analysed water samples.

that are sandwiched with lignite streaks, thin clay horizons and lenses at various locations (George *et al.* 2013). The thin clay/shale horizons truncate the vertical and lateral extents of the sandy aquifers, thereby building up sandy multi-aquifer systems in the area (Edet and Worden 2000). The presence of thin layers of argillaceous materials limits the current penetration depths predetermined by the characteristic absorption coefficient peculiar to the formation at higher frequencies, while the arenaceous materials of the depths of interest conduct current into the ground, thereby increasing depth of penetration at lower propagation frequencies.

3. Materials and methods

Fifteen resistivity measurements designed to capture prolific hydrogeological units in figure 1 were made using the SAS 4000 ABEM Terrameter employing Schlumberger electrode configuration. The apparent resistances were measured. The current cables were extended up to 1000 m in order to ensure that depths above 200 m were comfortably sampled assuming that exploration depth or depth of investigation varies between 0.25 and 0.5 of the current electrode separation (AB) (Roy and Elliot 1988; Singh 2000). Corresponding receiving (potential) electrode separation (MN) varied from a minimum of 0.5 m at AB = 2 m to a maximum of 50 m at AB = 1000 m. At all the electrode positions, care was taken to ensure that the separation between the potential electrodes did not exceed one fifth of the separation of the current electrodes (Gowd 2004). Transformation of the measured apparent resistance (Ra) to their corresponding apparent resistivity (ρ_a) was achieved by using the expression in equation (7):

$$\rho_a = \pi \cdot ((AB/2)^2 - (MN/2)^2/MN) \cdot Ra \quad (7)$$

The processed average geological resistivity and depth of investigation were combined with the associated pedotransfer function (PTF) used in EM method to establish the relationship between VES resolved depth of investigation and the EM resolved skin depth at their respective frequencies or period of energy penetration using equations (1 and 2).

4. Data analyses, results and discussion

In the reduction of electrical resistivity data from field data, manual and computer modelling techniques thrive (Zohdy 1966; Zohdy *et al.* 1977; George *et al.* 2011a, b) in realizing the equivalent 1-D geological models. The manual procedures involve plotting the field apparent resistivities on bi-logarithmic graphs, and where necessary, the curves generated were smoothened in order to remove the effects of lateral heterogeneities and other forms of noisy signatures (Bhattacharya and Patra 1966). This was performed by averaging the two readings at the cross-over points, or deleting any outlier at the cross-over points that did not conform to the dominant trend of the curve. Moreover, data that stood out as outliers in the prevalent curve trend, which could have caused serious increase in root mean square error (RMSE) during the modelling phase of the work, were also deleted. Such outliers, wherever observed, constituted less than 2% of the total data generated in each sounding station, and since we measured over 10 data per decade, deleting such noisy data did not alter the trend of the sounding curve. Some of the deleted data might have been the electrical signatures of the thin clay materials that might have suffered suppression from the over- and underlying thick sandy aquifers (Sabet 1975; Gurunadha Rao *et al.* 2011). Any discontinuity observed in the smoothened curves was exclusively attributed to vertical variation of electrical resistivity with depth. A computer-based VES modelling software called RESIST (Velpen Vender 1988), which can perform automated approximation of the initial resistivity model from the observed data, was later used to improve upon the preliminary interpreted results using the inversion technique (George *et al.* 2011a). The RESIST software uses the initial layer parameters to perform some calculations, and at the end, generates some theoretical data. It then compares the theoretical data with the field data. Since quantitative interpretation of geoelectrical sounding data is usually difficult due to the inherent problem of equivalence (Van Overmeeren 1988), borehole data were used to constrain the interpretations of all depths and minimise the choice of equivalent models by fixing layer thicknesses and depths while allowing the resistivities to vary (Batayneh 2000). The total number of observed minima and maxima on the smoothened VES curves were used as the models over a half space for the data inversion exercise. The software works iteratively by computing at the end of each step, updated parameters and the extent of fit between the calculated and the observed data. The RMSE technique in which 5% was preset as the maximum acceptable value was used in assessing the extent of fit. The borehole lithologic information obtained from the MDGP was juxtaposed with the nearby VES models. A good correlation was observed between the electrical resistivity derived 1-D models and the borehole lithologs. Examples of some modelled VES curves and their correlation with nearby borehole logs are

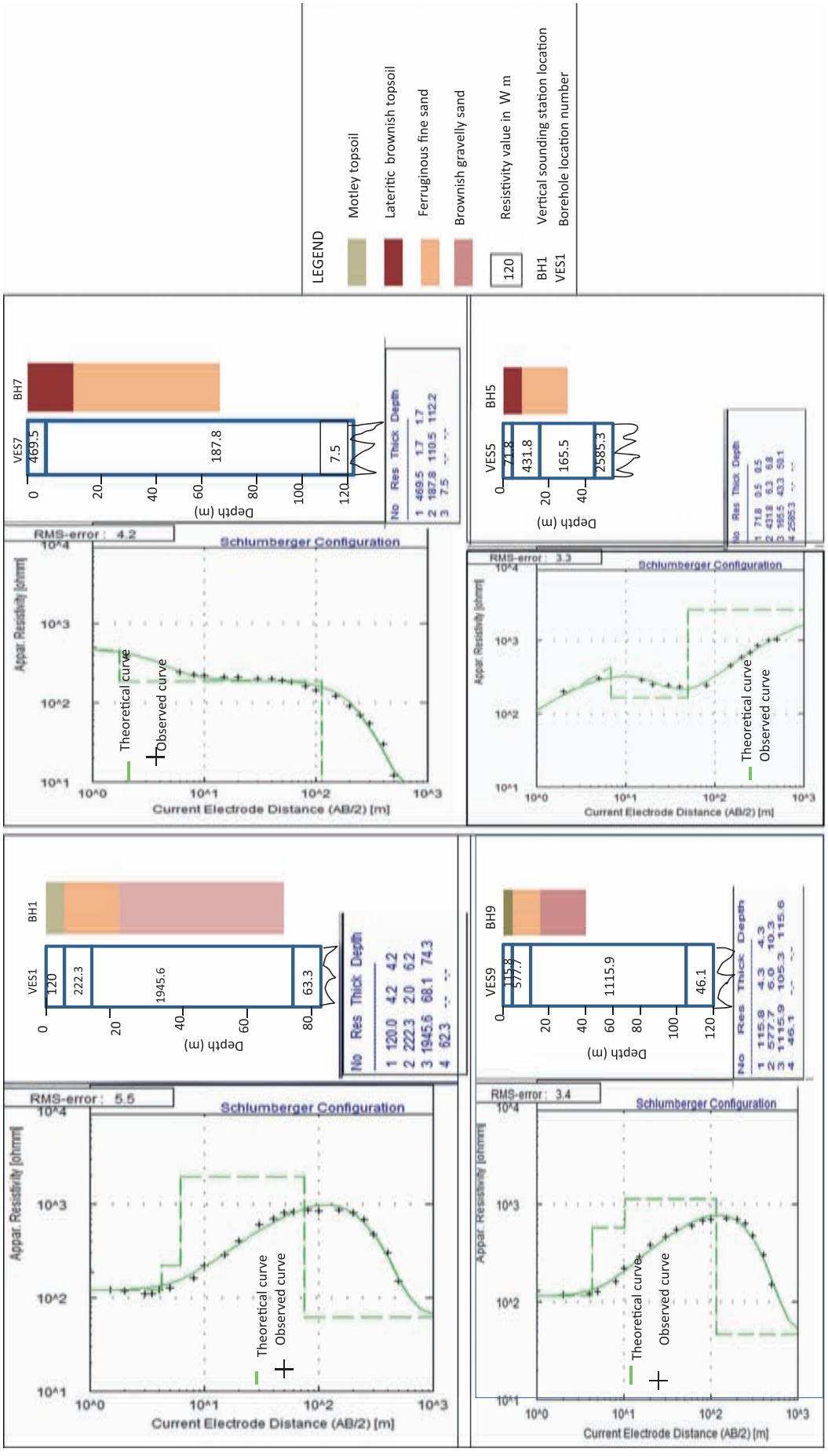

Figure 2. Model VES curves observed at VES 1, 5, 7 and 9. Insert: Correlation of borehole lithologs with inverted VES results.

shown in figure 2, which displays VES 1, 5, 7 and 9 and their corresponding boreholes. The three primary geoelectrical results, formation resistivities, formation thicknesses and formation depths, are presented in table 1. Three to four layers with AK ($\rho_1 < \rho_2 < \rho_3 > \rho_4$), H ($\rho_1 > \rho_2 < \rho_3$), KH ($\rho_1 < \rho_2 > \rho_3 < \rho_4$), and Q ($\rho_1 > \rho_2 > \rho_3$) curve types were penetrated and average resistivities to the depth of interest and their depths of penetrations used in comparing with the frequency dependent ac skin depth pedotransfer function are given table 2. A good correlation was observed between the borehole lithology logs and the inverted results over half space in many locations. In few stations, some minor misfits were noticed as the correlation was not quite good. These distortions were suspected to have possibly originated from the failure of the 1-D assumption of the shallow subsurface of the half space (Gurunadha Rao *et al.* 2011) and the equivalence and suppression problems, which the borehole data resolved.

From the electromagnetic skin depth transfer function, the effective and theoretical frequencies corresponding to the VES resolved average resistivity and depth of investigation were determined using frequencies corresponding to the skin depth, as seen in table 2. The theoretical frequency is directly proportional to the effective frequency but seems to be about 8.6 times higher in magnitude than the effective frequency from the diagnostic constant shown in the well-correlated (R_C = 0.9964) linear regression law governing the geological formation given in equation (8) (see figure 3).

$$F_T = 8.5511F_E + 496.36. \quad (8)$$

Table 1. *Summary of the results of geo-electric survey from computer modelling.*

VES	Lat. and Long. (degree)	No. of layers	Layer resistivity (Ωm)				Layer thickness (m)			Layer depth (m)			Curve type	Average lithologic description
			ρ_1	ρ_2	ρ_3	ρ_4	h_1	h_2	h_3	d_1	d_2	d_3		
1	4.56539N; 7.56056E	4	120.0	223.3	1945.6	62.3	4.2	2.0	68.1	4.2	6.2	74.3	AK	FS
2	4.56644N; 7.56147E	3	206.8	181.1	751.8	–	0.9	108.1	–	0.9	109.8	–	H	FS
3	4.56431N; 7.56081E	3	873.2	71.3	2332.5		5.1	81.1	–	5.1	86.2	–	H	FS
4	4.56572N; 7.55981E	3	1020.6	735.5	1465.9	–	7.6	87.7	–	7.6	95.3	–	H	FS
5	4.56702N; 7.55713E	4	71.8	431.8	165.5	2858.3	0.5	6.3	43.3	0.5	6.8	50.1	KH	FS
6	4.56594N; 7.55675E	3	554.2	362.2	1888.4	–	11.3	170.4	–	11.3	181.7	–	H	FS
7	4.56322N; 7.56177E	3	469.5	187.8	7.5	–	1.7	110.5	–	1.7	112.2	–	Q	FS
8	4.66768N; 7.56567E	3	392.5	197.7	74.9	–	2.4	51.9	–	2.4	54.2	–	Q	FS
9	4.56237N; 7.56322E	4	115.8	577.7	1115.9	46.1	4.3	6.0	105.3	4.3	10.3	115.6	AK	FS
10	4.67754N; 7.56965E	3	403.5	203.8	127.8	–	1.4	30.9	–	1.4	32.3	–	Q	FS
11	4.55634N; 7.56786E	4	90.5	396.7	8.2	25.3	1.0	5.4	94.5	1.0	6.4	100.9	KH	FS
12	4.56566N; 7.56656E	4	660.4	1488.6	549.2	1248.7	1.3	3.6	47.8	1.3	4.9	52.7	KH	FS
13	4.56452N; 7.56023E	4	205.8	750.3	52.6	66.8	2.9	11.8	66.2	2.9	14.7	82.9	KH	FS
14	4.55867N; 7.56734E	4	210.7	397.9	1721.4	228.2	0.7	12.8	55.2	0.7	13.5	68.2	AK	GS
15	4.55945N; 7.56776E	4	136.4	809.6	24.2	166.3	0.7	2.6	74.9	0.7	3.4	78.2	KH	FS

Note: GS = Gravelly Sand; FS = Fine Sand.

Table 2. *Summary of generated parameters between VES and EM pedotransfer functions.*

VES	Average resistivity resolved from VES (Ωm)	Average conductivity resolved from VES (S/m)	Average VES resolved depth (m)	Average equivalent EM resolved depth at indicated frequency (m)	Effective frequency from EM PTF at the indicated depth (Hz)	Corresponding EM theoretical frequency at the indicated VES depth (Hz)
1	762.97	0.001311	74.3	71.31947	1500	12713.78
2	193.95	0.005156	109.8	110.0994	160	1479.892
3	472.25	0.002118	86.2	88.71772	600	5846.585
4	878.05	0.001139	95.3	96.13861	950	8893.614
5	223.03	0.004484	50.1	51.22385	850	8173.963
6	458.2	0.002182	181.7	174.776	150	1276.704
7	328.65	0.003043	112.2	122.2237	220	2401.556
8	295.1	0.003389	54.2	54.32311	1000	9240.925
9	603.2	0.001658	115.6	115.7776	450	4152.317
10	303.65	0.003293	32.3	31.81457	3000	26773.99
11	165.13	0.006056	100.9	104.9222	150	1492.067
12	254.7	0.003926	52.7	51.77888	750	8436.31
13	536.2	0.001865	82.9	81.8688	800	7177.324
14	1721.4	0.000581	68.2	65.60107	4000	34045.36
15	32.34	0.030921	78.2	76.68116	55	486.4871

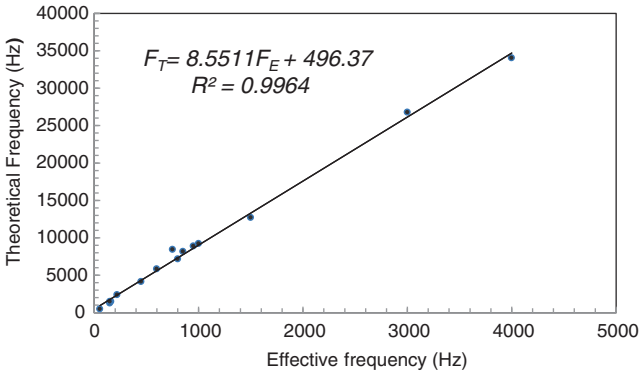

Figure 3. A plot showing the relationship between theoretical and effective frequency of EM obtained through VES pedotransfer function.

The diagnostic relation shows that the theoretical frequency is about 8.6 times elevated, than the effective frequency. Although this expression is site dependent due to the compositions of the geological formation, it gives a clue to the behaviour of frequencies at the investigated depth and the associated energy loss factor. The penetrating frequency depends on the electrical resistivity, ρ, and the energy of the injected current, I, and voltage, V, as in the expression

$$\rho = \frac{1}{\sigma} = K\frac{\Delta V}{I}. \tag{9}$$

For a given geometric constant, K, in equation (9), resistivity or conductivity can be written in terms of electrical energy and frequency as given by equation (10):

$$\rho = KQVf = K\beta f$$

or

$$f = \frac{\rho}{K\beta} = \frac{1}{\sigma K\beta}, \tag{10}$$

where Q the electric charge is in coulomb and $QV = \beta$ is the electrical energy measured in Joules. The expression in equation (11) shows that frequency is directly proportional to resistivity and inversely proportional to electrical energy of the injected current. This signifies that at large current/energy, the frequency reduces and large penetration depth is enhanced depending on the absorption/attenuation coefficient of the geological formation, which on the average, increases exponentially with source frequency of the penetrating source (see figure 4). The loss factor, Γ, increases with formation conductivity and depth, while frequency decreases with increasing loss factor, as the study shows in figure 5. However, with constant energy loss factor, the frequency increases with conductivity – the reason for having a definitive geometry of a conductive geological formation at higher frequencies. When the power/energy loss factor increases, the frequency reduces and the exploration depth increases. In this condition, the geometry of the delineated formation may not be appropriately definitive as compared to higher frequencies with shallow exploration depths. Generally, the depth of

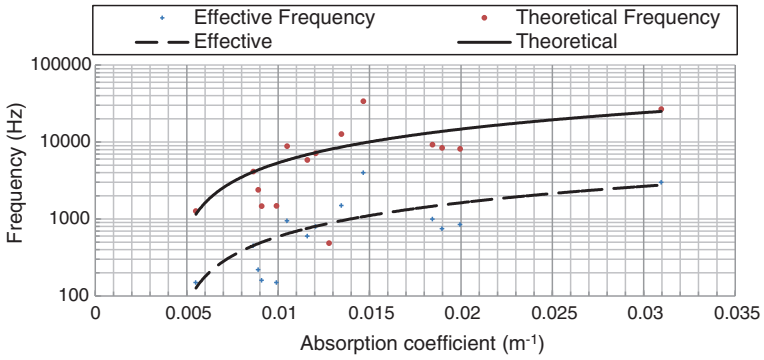

Figure 4. A plot of frequency against the inferred absorption coefficient.

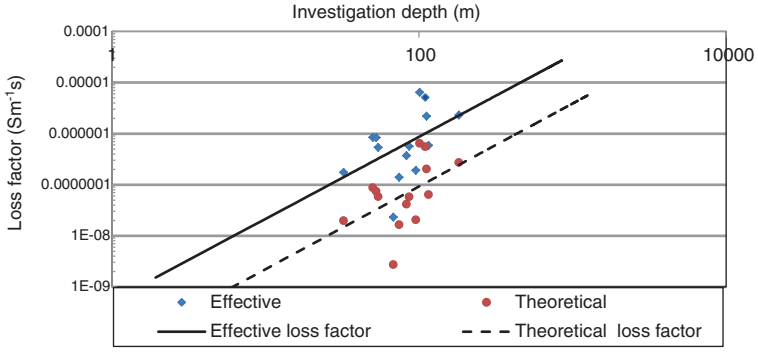

Figure 5. A plot of loss factor against investigation depth.

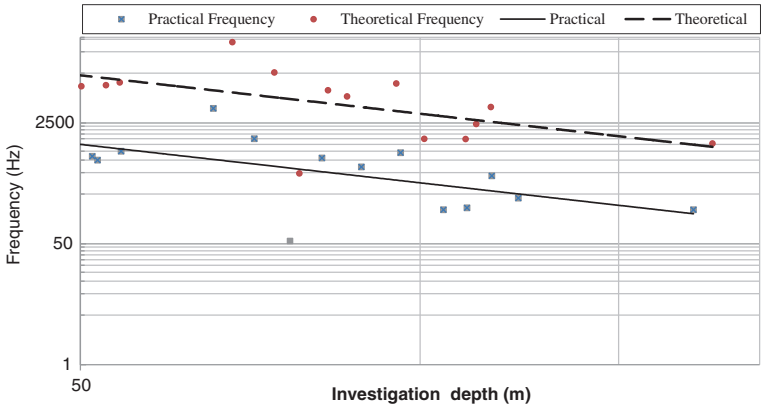

Figure 6. A plot of frequency against investigation depth.

investigation, as inferred in figure 6, decreases with increasing frequency, and this suggests that the loss factor of the injected energy and the absorption coefficient in the geological resource of interest increases with depth. As displayed in figure 7, effective and theoretical frequencies increase with average resistivity in the sandy fine sand formation under study. In the linear regression relations, equations (11 and 12), respectively, represent the power laws governing the fine sand formation for the theoretical and effective frequencies, corresponding to the VES resolved depths of investigation considered.

$$F_T = 24.537\rho^{0.9104} \tag{11}$$

$$F_E = 2.8491\rho^{0.8982} \tag{12}$$

From equations (11 and 12), the ratio of the diagnostic coefficient $\left(24.537\ \mathrm{Sm^{-1}s^{-1}}\right)$ of $F_T - \rho$ plot to $\left(2.8491\ \mathrm{Sm^{-1}s^{-1}}\right)$ of $F_E - \rho$ plot gives a constant

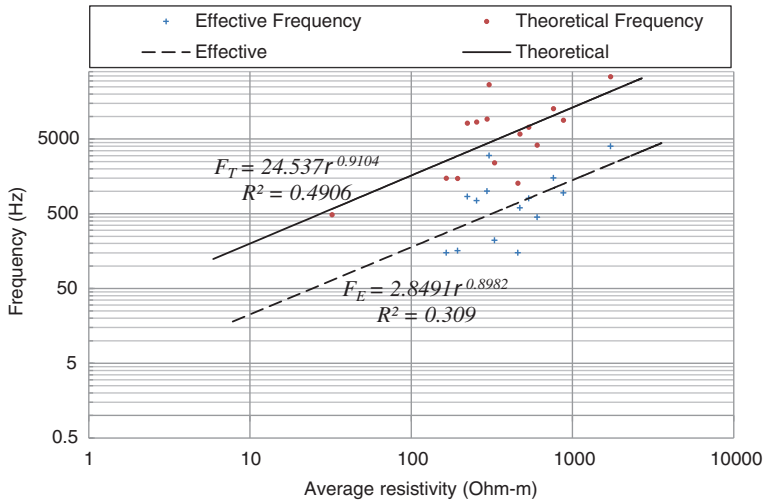

Figure 7. A plot of frequency against average resistivity.

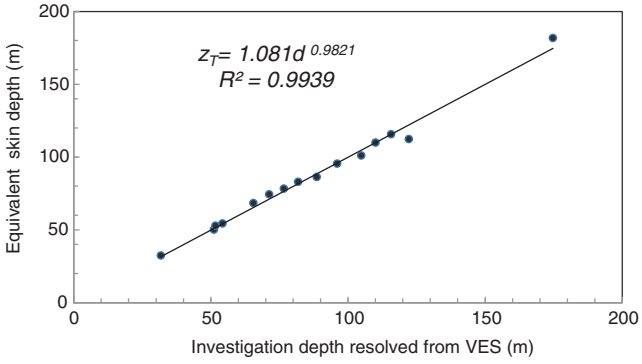

Figure 8. A plot of equivalent skin depth against VES resolved depth.

value of about 8.6, which is the multiplicative factor that can be used to convert effective frequency to theoretical frequency. The powers of the diagnostic constants are similar indicating the uniqueness and homogeneous and isotropic nature of the geological formation in the considered depth of exploration. However, the correlation coefficients that are less than five indicate the presence of minor gravelly sands in the fine sands. These diagnostic relations are paramount in predicting the frequency/period, loss factor, attenuation/absorption coefficient and the energy of the injected signal. The relations are also useful in estimating the electrical resistivity/conductivity, which can easily be measured in geoelectrical surveys. The PTF in geoelectrical measurements were used to estimate the EM resolved skin depth at their corresponding frequencies. The resolved VES depths of investigation, d, and the equivalent EM resolved depths obtained from effective depths of penetration, ς_T, were plotted as presented in figure 8. The plot shows a proportional relation between VES and EM resolved depths at the indicated frequencies with high correlation coefficient ($R_c = 0.9939$), as expressed in the Power law in equation (13).

$$\varsigma_T = 1.081d^{0.9821} \tag{13}$$

This Power law can be used to constrain the interpretation of VES resolved depth at a given resistivity/conductivity of effective known frequency, when the effective skin depth is available. The comparison between the VES and EM resolved depth spreads are shown in the contour map in figure 9. The contour shows a good spread resemblance of depth of exploration between the VES and EM resolved PTFs. Box plot is a statistical technique, which is commonly used as a standard statistical tool and can be used in presenting a 5-number summary of a dataset distribution (Pfannkuch 2006). The dataset summary includes the minimum, the lower quartile, the median value, the upper quartile and the maximum value. The ranges of exploration depth from VES and EM PTFs are unique, thereby showing the goodness of fit at the indicated frequencies in figure 10. The respective minimum (32.3, 31.8 m), maximum (181.7, 174.8 m) and the average (86.3, 86.4 m) exploration depths for the VES and EM PTFs are correspondingly in tune. This implies that at appropriate frequency, the non-uniqueness in the interpretation of VES data can be enhanced through the use of EM PTFs. It is observable through the analysis that there is a great departure between the effective and theoretical frequencies, by a factor of about 8.6. The ranges of frequency distributions between the effective (minimum = 55 Hz; maximum = 4000 Hz; average = 975.7 Hz) and the theoretical (minimum = 486.5 Hz; maximum = 34045.4 Hz; average = 8839.4 Hz) EM penetration depths are wide, as shown in the box plot of

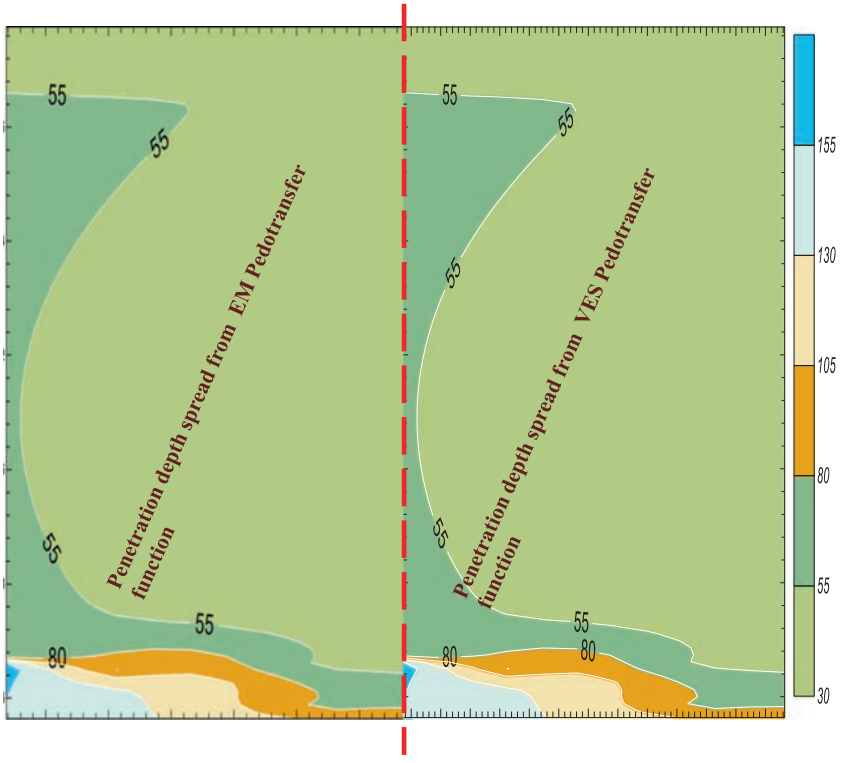

Figure 9. Contour map showing the spread in EM and VES resolved depths of investigation with discontinuous line showing the boundary.

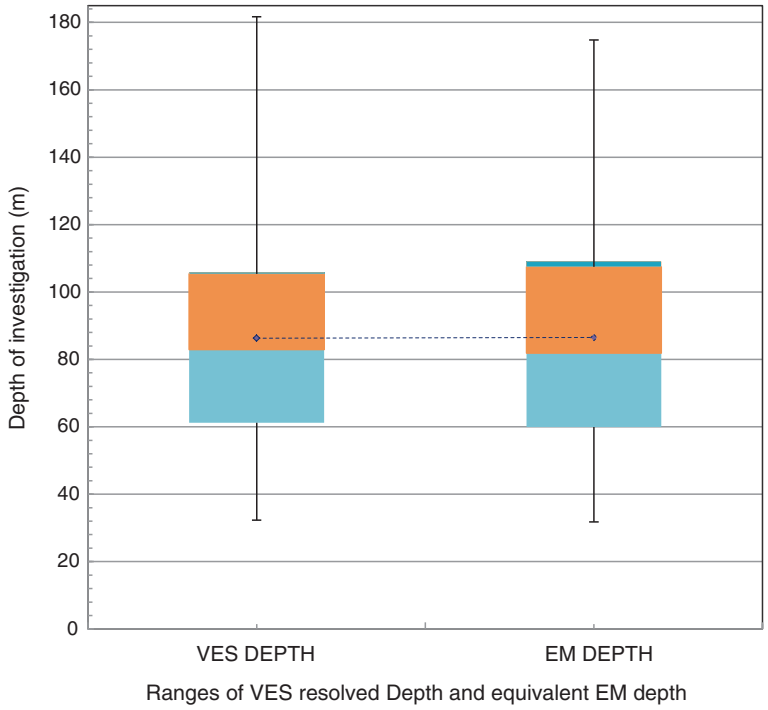

Figure 10. Box plot showing the ranges of depth of exploration obtained from combination of VES and EM PTFs with colour bands from bottom to top respectively showing the difference between median and lower quartile and upper quartile and median.

figure 11. This departure could cause anomalous interpretations. Therefore, the effective depth in which a geological formation lies and still be recognizable should, as a matter of fact, be located through the use of adequate signal source period or frequencies. However, the theoretical frequency

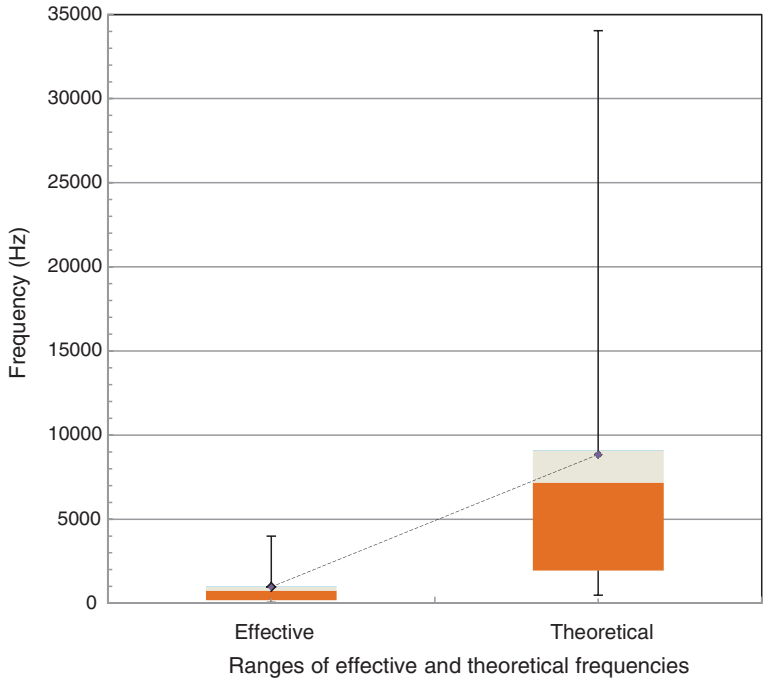

Figure 11. Box plot showing the ranges of effective and theoretical frequencies obtained from combination of VES and EM PTFs with colour bands from bottom to top respectively showing the difference between median and lower quartile, and upper quartile and median.

should always be converted to effective frequency using the transfer function, in order to arrive at the targeted depth of investigation of interest with high fidelity.

5. Conclusion

The pedotransfer function of EM skin depth, i.e., the depth at which the amplitude of a frequency domain electromagnetic field source falls to e^{-1} of its value at the surface of a homogeneous half space, is compared with the 1-D current electrical resistivity model parameters, which includes average electrical resistivities and depths of current penetration of economic hydrogeological units at chosen frequencies corresponding to the VES resolved penetration depths. The depth of penetration/skin depth, which is predetermined by skin effect, depends on loss factor, absorption/attenuation coefficient and average frequency/period of subsurface down to that depth of known average resistivity/conductivity of interest from the top layer (Hersir and Flóvenz 2013). The frequencies corresponding to theoretical and effective depth of penetration associated with EM field were considered. The results show that the frequency of EM source theoretical skin depth corresponding to the VES resolved exploration depth is about 8.6 times that of the effective depth of penetration, therefore showing a wide departure between effective and theoretical frequencies. Peculiar governing pedotransfer functions/relations have been established through the use of statistical regression analysis. The ranges and distributions of the estimated parameters have been established using appropriate tools, such as contour and box plot. Based on the novel diagnostic relations and their corresponding constants between VES data and EM skin depth transfer function, checking for the accuracy associated with the non-unique interpretations that characterise the 1-D resistivity data can be enhanced, mostly when lithostratigraphic data are not available.

References

Akpan A E, George N J and George A M 2000 Geophysical investigation of some prominent gully erosion sites in Calabar, southeastern Nigeria and its implications to hazard prevention; *Disaster Advances* **2(3)** 46–50.

Batayneh A T 2000 A hydrogeophysical model of the relationship between geoelectric and hydraulic parameters, central Jordan; *J. Water Resour. Protect.* **1** 400–407.

Bhattacharya P K and Patra H P 1966 *Direct current geoelectric sounding: Principles and interpretation*; Elsevier Science Publishing Co. Inc.

Bostick F X 1977 A simple almost exact method of MT analysis, Workshop on electrical methods in geothermal exploration; *US Geol. Surv.,* Contract no. 140800018-359.

Edet A E and Worden R H 2000 Monitoring of the physical parameters and evaluation of the chemical composition of river and groundwater in Calabar (southeastern Nigeria); *Environ. Monit. Assess.* **157** 243–258.

George N J, Akpan A E and Obot I B 2011a Resistivity study of shallow aquifer in parts of southern Ukanafun

Local government area, Akwa Ibom State; *E-J. Chemistry* **7(3)** 693–700.

George N J, Emah J B and Ekong U N 2011b Geohydrodynamic properties of hydrogeological units in parts of Niger Delta, southern Nigeria; *J. Afr. Earth Sci.* **105** 55–63.

George N J, Akpan A O and Umoh A 2013 Preliminary geophysical investigation to delineate the groundwater conductive zones in the coastal region of Akwa Ibom State, southern Nigeria, around the Gulf of Guinea; *Int. J. Geosci.* **4** 108–115.

George N J, Nathaniel Ekong U and Etuk S E 2014a Assessment of economically accessible groundwater reserve and its protective capacity in Eastern Obolo Local Government Area of Akwa Ibom State, Nigeria, using electrical resistivity method; *ISRN Geophysics* **2014** 1–10.

George N J, Ubom A I and Ibanga J I 2014b Integrated approach to investigate the effect of leachate on groundwater around the Ikot Ekpene Dumpsite in Akwa Ibom State, southeastern Nigeria; *Int. J. Geosci.* **2014** 1–10.

George N J, Ibanga J I and Ubom A I 2015 Geoelectrohydrogeological indices of evidence of ingress of saline water into freshwater in parts of coastal aquifers of Ikot Abasi, southern Nigeria; *J. Afri. Earth Sci.* **109** 37–46.

Gowd S S 2004 Electrical resistivity surveys to delineate groundwater potential aquifers in Peddavanka watershed, Anantapur District, Andhra Pradesh, India; *Environ. Geol.* **46** 118–131.

Gurunadha Rao V V S, Tamma Rao G, Surinaidu L, Rajesh R and Mahesh J 2011 Geophysical and geochemical approach for seawater intrusion assessment in the Godavari Delta Basin, A.P., India; *Water Air Soil Poll.* **217** 503–514.

Hersir G P and Flóvenz Ó G 2013 Resistivity surveying and electromagnetic methods, *Global Environment*, IGA Academy Report 0110–2013.

Karim H H and Al-dami H A N 2012 GPR data simulation for detecting subsurface bodies; *Eng. Tech. J.* **30(15)** 2677–2693.

Kearey P and Brooks M 2002 *An Introduction to Geophysical Exploration*, Blackwell; 3rd edn; Scientific Publications Ltd, London.

Keller G V 1971 Natural-field and controlled-source methods in electromagnetic exploration; *Geoexploration* **9** 99–147.

Parasnis D S 1979 *Principles of Applied Geophysics,* Chapman and Hall, 275p.

Parker R L 1982 The existence of a region inaccessible to magnetotelluric sounding; *Geophys. J. Roy. Astr. Soc.* **68** 165–170.

Pfannkuch M 2006 Comparing box plot distributions: A teacher's reasoning; *Edu. Res. J.* **5(2)** 27–45.

Reid J E and Macnae J C 1999 Doubling the effective skin depth with a local source; *Geophysics* **64** 732–738.

Reijers T J A and Petters S W 1988 Depositional environment and diagenesis of Albian carbonates in Calabar Flank, SE Nigeria; *J. Petrol. Geol.* **10** 283–294.

Reijers T J A, Petters S W and Nwajide C S 1999 The Niger Delta Basin; In: *African Basins – Sedimentary Basin of the World 3,* Elsevier Science, Amsterdam, pp. 151–172.

Roy K K and Elliot H M 1988 Some observations regarding depth of exploration in DC electrical methods; *Geoexploration* **19** 1–13.

Sabet M A 1975 Vertical electrical resistivity sounding locate groundwater resources: A feasibility study. Virginia Polytechnical Institute; *Water Resour. Bull.* **73** 63.

Schuylenbergh K V and Puers R 2009 *Inductive Powering: Basic Theory and Application to Biomedical Systems*; Springer Science & Business Media, 223p.

Singh K P 2000 Nonlinear estimation of aquifer parameters from surficial resistivity measurements; *J. Hydrol. Earth Syst. Sci. Discuss.* **2** 917–938.

Singh N P and Mogi T 2003a Effective skin depth of EM fields due to large circular loop and electric dipole sources; *Earth Planets Space* **55** 301–313.

Singh N P and Mogi T 2003b EMLCLLER – A program for computing the EM response of a large loop source over a layered earth model; *Comput. Geosci.* **29(10)** 1301–1307.

Spies B R 1989 Depth of investigation in electromagnetic sounding methods; *Geophysics* **54** 872–888.

Stratton J A 1941 *Electromagnetic Theory*; McGraw-Hill Book Co., New York.

Van Overmeeren R 1988 Aquifer boundaries explored by geoelectrical measurements in the coastal plain of Yemen: A case study of equivalence; *Geophysics* **54** 38–48.

Velpen Vender B P A 1988 A computer processing package for D.C. resistivity interpretation for an IBM compatibles; *ITC Journal 4*, The Netherlands.

Zohdy A A R 1966 The auxiliary point method of electrical sounding interpretation and its relationship to the Dar-Zarrouk parameters; *Geophysics* **30** 644–660.

Zohdy A A R, Eaton G P and Mabey D R 1977 Application of surface geophysics to groundwater investigation; *USGS Techniques of water resources investigations*, Book 2, Chapter D1 116.

MS received 7 January 2016; revised 3 April 2016; accepted 10 June 2016

Corresponding editor: Pawan Dewangan